JOURNAL OF MAGNETIC RESONANCE **133,** 104–114 (1998)
ARTICLE NO. MN981422

Optimizing the ^{13}C–^{14}N REAPDOR NMR Experiment: A Theoretical and Experimental Study

Yong Ba,* Hsien-Ming Kao,* Clare P. Grey,*,[1] Lamy Chopin,† and Terry Gullion‡,[1]

Chemistry Department, SUNY Stony Brook, Stony Brook, New York 11794-3400; †Department of Chemistry, Florida State University, Tallahassee, Florida 32306; and ‡Department of Chemistry, West Virginia University, Morgantown, West Virginia 26506

Received July 18, 1997; revised February 19, 1998

The optimum ^{14}N pulse lengths in the ^{13}C–^{14}N rotational-echo adiabatic-passage double-resonance (REAPDOR) NMR experiment are determined from calculations and from experiments on samples of glycine and L-alanine. The REAPDOR experiment utilizes the adiabatic passages that ^{14}N spins make between the ^{14}N Zeeman energy levels during the application of a single, short ^{14}N radiofrequency pulse. Use of a short ^{14}N irradiation time of less than one-quarter of a rotor period ensures that the number of ^{14}N spins that undergo more than one passage is minimized. This simplifies calculations describing ^{13}C dipolar dephasing and provides better agreement between calculations and experiments. Recovery of the ^{13}C–^{14}N dipolar couplings and ^{14}N quadrupolar coupling constants and asymmetry parameters is described.

Key Words: **NMR; REAPDOR; double resonance; nitrogen.**

INTRODUCTION

Rotational-echo, adiabatic-passage, double-resonance NMR (REAPDOR) is an experiment designed to recover the heteronuclear dipolar coupling between spin-1/2 and quadrupolar nuclei (*1*, *2*). This experiment combines the attractive features of the rotational-echo, double-resonance NMR (REDOR) (*3*, *4*) and the transfer-of-populations, double-resonance NMR (TRAPDOR) experiments (*5*–*7*). The ^{13}C–^{14}N REAPDOR pulse sequence is shown in Fig. 1. A pulse train of π pulses is applied to the spin-1/2 nuclei (^{13}C) during the dipolar evolution period of N_c rotor cycles, and a single, short RF ''adiabatic-passage pulse'' of length τ is applied to the quadrupolar nuclei (^{14}N) in the middle of the dipolar evolution period. The spacing between adjacent π pulses is one-half of a rotor period; no π pulse is applied at the midpoint of the experiment so that the ^{13}C chemical shift anisotropy is refocused at the beginning of data acquisition. This π-pulse train causes dipolar dephasing of ^{13}C spins coupled to ^{14}N spins to occur during the first half of the evolution period. When the adiabatic-passage pulse is omitted, the average dipolar dephasing for the two halves of the dipolar evolution period are opposite in sign, and the dipolar interaction is refocused; this produces the full signal, S_m, which accounts for T_2 decay. However, when the adiabatic-passage pulse is applied, the populations of the ^{14}N spins within the eigenstates are interchanged. This alters the dipolar dephasing of the ^{13}C spins and the transverse magnetization is no longer fully refocused, resulting in a reduced signal. The difference signal, ΔS_m, is generated by subtracting the reduced signal from the full signal. The heteronuclear dipolar interaction can be recovered from the ratio of ΔS_m and S_m.

Applications of the experiment to recover ^{13}C–^{14}N and ^{13}C–^{17}O heteronuclear–dipolar couplings have recently been demonstrated (*1*, *2*). Preliminary ^{13}C–^{14}N experimental results on a sample of L-alanine that had been diluted with ^{15}N nuclei were reported in Ref. (*1*), and the data were compared with a theoretical REAPDOR dephasing curve. In this paper, we provide a more detailed description of the theory and optimized experimental conditions for the REAPDOR experiment. Calculated REAPDOR dipolar dephasing curves are compared to those obtained experimentally under a variety of different conditions. The dependence of the REAPDOR experiment on spinning speed, RF (radio frequency) power, and length of the adiabatic-passage pulse is explored for samples of glycine and alanine. Finally, the REAPDOR experiment is used to determine the quadrupolar coupling constants and the asymmetry parameters for spin-1 nuclei.

ADIABATIC PASSAGES

The quadrupolar interaction is time dependent under MAS and changes sign two or four times per rotor period, depending on the relative orientation of the quadrupolar principal axes and the axis of sample rotation. Although the eigenvalues of the quadrupolar nuclei change as the sample rotates, the eigenstates remain unchanged. Application of a close-to-on-resonance RF field to the quadrupolar nuclei during the sample spinning, however, may result in population interconversions between the eigenstates at every change in the sign of the quadrupolar splitting, Q (i.e., a zero-crossing of Q).

The effects of the ^{14}N zero crossings on the ^{14}N spin populations can be seen by plotting the ^{14}N eigenvalues as a function of Q/ω_1 (Fig. 2). Three different ratios of the fre-

[1] To whom correspondence should be addressed.

1090-7807/98 $25.00

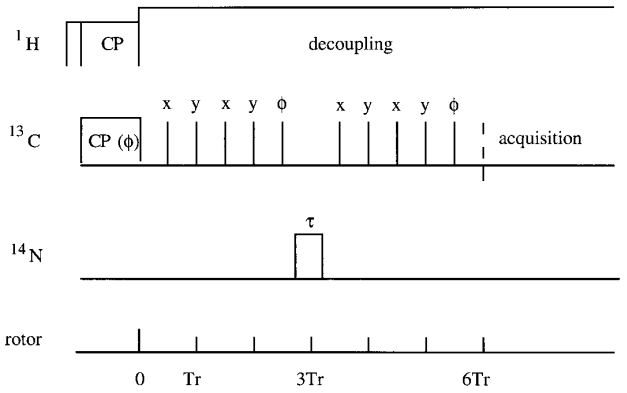

FIG. 1. The $^{13}C/^{14}N$ REAPDOR pulse sequence for $N_c = 6$ (6 rotor periods). ^1H to ^{13}C cross-polarization is immediately followed by the dipolar evolution period of N_c rotor cycles. Two sets of strings of XY-4π pulses are applied to the ^{13}C channel during this time. Each string of XY-4 pulses is followed by a π pulse of phase ϕ (the phase of the transverse ^{13}C magnetization at the end of the spin-locking pulse), that is, at $(N_c - 1)T_r/2$ and $(2N_c - 1)T_r/2$. Signal acquisition immediately follows the dipolar evolution period. The experiment is then repeated omitting the ^{14}N pulse (the control experiment).

quency offset of the applied irradiation, δ, to the RF amplitude, ω_1, are shown which correspond to on-resonance, close-to-on-resonance, and off-resonance conditions, respectively (*6*). For the $\delta/\omega_1 = 0$ condition, the $|0\rangle$ eigenstate and the mixed state $\{|+1\rangle + |-1\rangle\}$ are connected, and avoided level crossings are observed at the zero crossing of Q. Transfer of populations between the $|0\rangle$ eigenstate and the double-quantum coherence results. For off-resonance irradiation, the avoided level crossings occur at $Q = \pm 2\delta$. However, when the irradiation is close to on-resonance ($\delta/\omega_1 \approx 1$), these are very close to the zero crossings in Q. Since the width of these crossings is of the order of ω_1, two separate avoided level crossings cannot be distinguished, and the eigenstates $|+1\rangle$, $|0\rangle$, and $|-1\rangle$ continuously evolve into their connected eigenstates when Q changes sign (*6*). Mixed states are observed at the zero crossings of Q. In contrast, when the RF irradiation frequency is applied further from resonance such that $\delta > \omega_1$ (e.g., $\delta/\omega_1 = 5$), two separate avoided level crossings can now be discerned at $Q = \pm 2\delta$. When Q passes through the condition $Q = -2\delta$, the eigenstates $|0\rangle$ and $|+1\rangle$ are converted to $|+1\rangle$ and $|0\rangle$, respectively, whereas when Q passes through the second avoided level crossing (at $Q = +2\delta$), the eigenstates $|0\rangle$ and $|-1\rangle$ are converted into $|-1\rangle$ and $|0\rangle$, respectively. Thus, the conversion of the $|+1\rangle$ eigenstate to the $|-1\rangle$ eigenstate (for $-Q$ to $+Q$) occurs via two separate single-quantum avoided level crossings, the eigenstate $|0\rangle$ existing as an intermediate for values of Q close to zero (i.e., close to the zero crossings in Q).

Under conditions of a weak RF field, fast sample rotation, or for a very large quadrupolar coupling constant (QCC) (i.e., when the passages are far from adiabatic), the system will be unaffected by the crossings and the spin populations will remain in the same eigenstates after the crossings. For intermediate conditions, significant spin populations are transferred to a linear combination of wavefunctions and the system may not necessarily return to its initial condition after a complete rotor cycle. An adiabaticity parameter, $\alpha = \omega_1^2/\omega_r\omega_Q$, has been defined for a powder, where ν_r is the sample rotation frequency and $\omega_Q = 3QCC/[2I(2I - 1)]$ is the quadrupolar frequency (*8*). The adiabaticity parameter provides an estimate of how close the passages between eigenstates are to being adiabatic. Adiabatic passages are predicted for $\alpha \gg 1$. In practice, however,

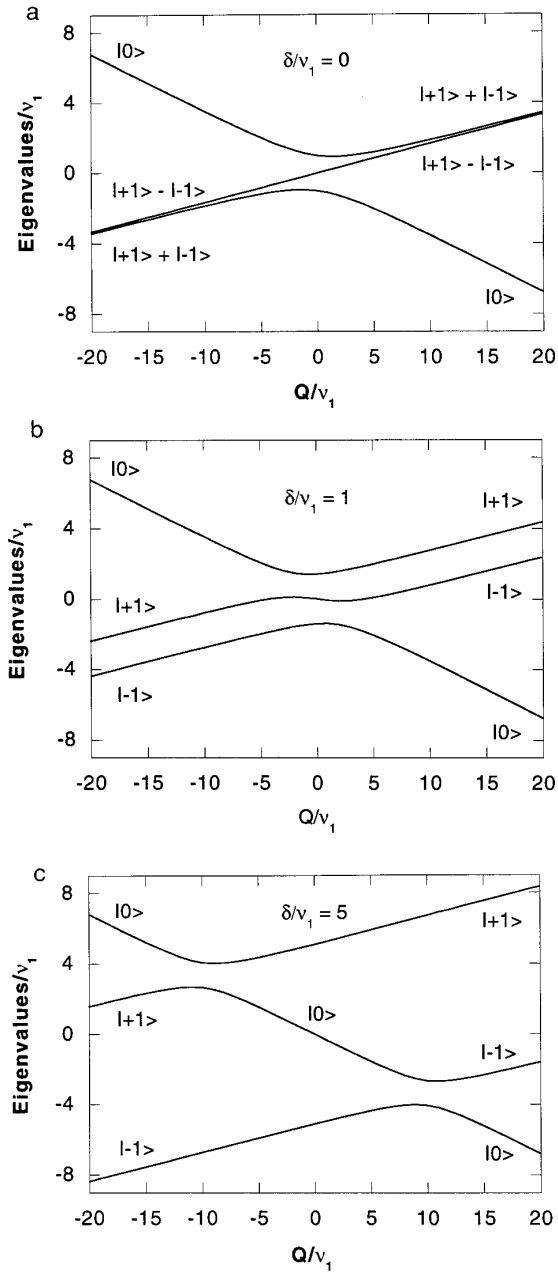

FIG. 2. The change in $I = 1$ eigenvalues with quadrupole splitting, Q, for $\delta/\nu_1 = 0$ (a), 1 (b), and 5 (c). The eigenstates at large values of Q/ν_1, and for $Q = 0$ in (c), are indicated.

significant population transfers between eigenstates have been observed for values of α noticeably less than 1 (*7, 11, 12*). These avoided level crossings of the eigenstates of quadrupolar nuclei, and their effect on spin-locking, cross-polarization dynamics, and double resonance experiments, have been described in detail for $I = 1$, 3/2 and 5/2 nuclei (*5–11*).

Population transfers are used in both the TRAPDOR (*5–7*) and REAPDOR (*1, 2*) experiments to recover the dipolar interaction between spin-1/2 nuclei and quadrupolar nuclei under conditions of MAS. Since the quadrupolar nuclei are irradiated during the whole dipolar-evolution period in the TRAPDOR experiment, the RF irradiation must be applied for multiple rotor periods if a weak heteronuclear dipolar coupling is to be detected. Hence, a large number of zero crossings will occur. Even under conditions of slow MAS and high RF field strengths, the passages may not be adiabatic for all of the spins in the sample, and it becomes very difficult to predict and calculate the effect of multiple nonadiabatic passages. This problem increases geometrically as the number of passage attempts increases. The extent of population transfer after nonadiabatic passages has been calculated numerically and semiempirically for a two-level spin system (*7, 10*). Those calculations have been used to calculate the population transfers for $I = 5/2$ spin systems when $\delta > \nu_1$ (*7*). However, one problem that still remains to be adequately addressed is how to determine the effect of the non-spin-locked coherences (i.e., the linear combinations of wavefunctions) on the subsequent passages. Although a numerical calculation for one spin with one orientation in the powder is straightforward, a calculation for the whole powder, while feasible (*13*), is computer intensive. Thus, in calculations of the dephasing in the TRAPDOR experiment, the non-spin-locked coherences have either been assumed to be so rapidly oscillating under the quadrupolar Hamiltonian that they do not contribute to the dephasing of the dipolar-coupled *S* spin, or these coherences decay rapidly so that any possible refocusing of these coherences is ignored (*7*). One of the major advantages of the REAPDOR experiment is that the number of passages any spin attempts is very limited; consequently, the effect of the adiabatic-passage pulse on the dipolar dephasing should be simpler to calculate.

The fraction of spins, in a powder sample, that make zero crossings during the adiabatic-passage pulse has been calculated numerically as a function of the rotor fraction of the ^{14}N RF irradiation (i.e., the adiabatic-passage pulse length). These results are shown in Fig. 3, where the fraction of spins that make no, single, double, triple, quadruple, and an odd number of zero crossings are plotted. The position of each zero crossing in the rotor period was determined by solving, with MATHEMATICA, the equation $Q(t) = 0$ (from (*14*)) for explicit values of α, β, and γ (the Euler angles describing the relative orientations of the quadrupolar, rotor, and static magnetic field frames). Calculations were performed for the powder by averaging over all α, β, and γ in steps of 2° for $\eta = 0$ and in steps of 6° for $\eta = 0.54$ and 1.0. The $\eta = 0.54$ value is

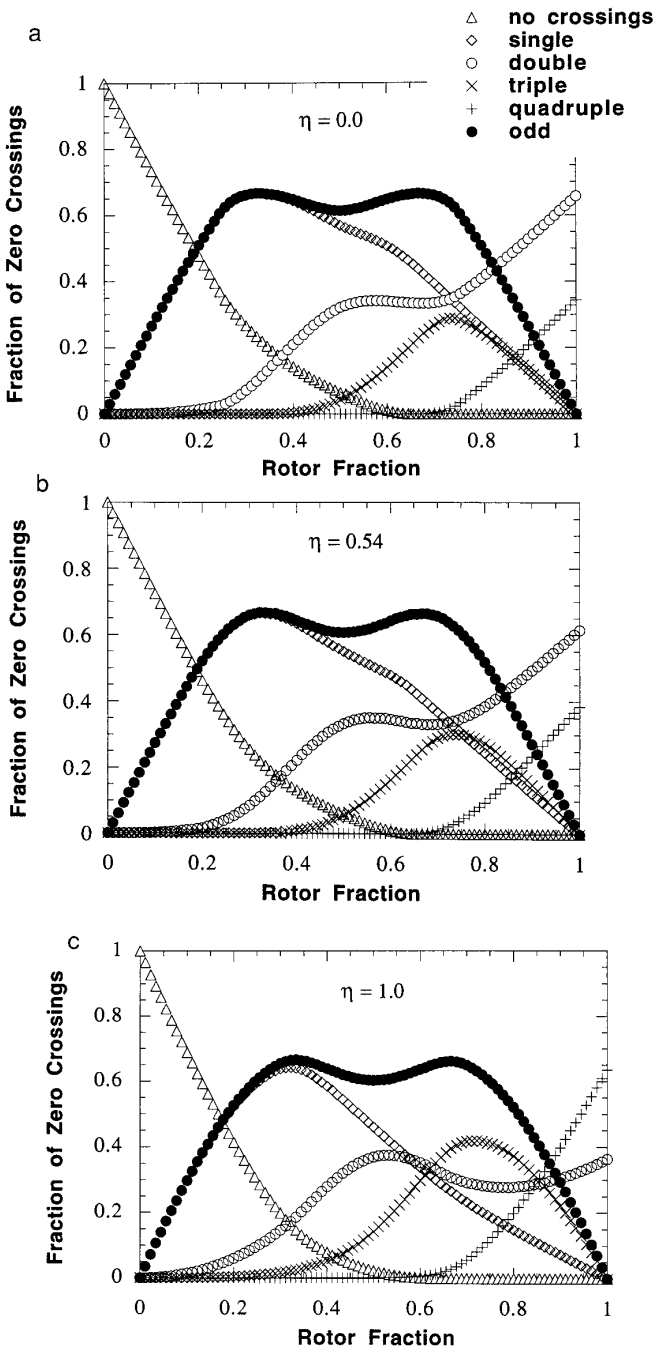

FIG. 3. The calculated fractions of spins that have undergone zero crossings, as a function of the ^{14}N irradiation time. The fractions of spins that have undergone no, single, double, triple, quadruple, and an odd number of zero crossings are plotted for values of η = (a) 0.0, (b) 0.54, and (c) 1.0.

shown specifically since it is the measured asymmetry parameter for glycine (*14*). For very short irradiation times, only the fraction of spins making single zero crossings is significant, the fractions of double, triple, and quadruple zero crossings increasing at longer irradiation times. The fraction of spins making a single adiabatic passage increases until it reaches a

maximum at one-third of a rotor period. At the end of one rotor period, the fractions of single and triple zero crossings have returned to zero while the fractions of double and quadruple zero crossings have reached their maximum values. The fraction of odd numbers of zero crossings are symmetric about $T_r/2$ for all values of η.

Although the fraction of ^{14}N spins making odd numbers of zero crossings is independent of η, the fraction of single crossings is not. The fractions of single and odd crossings remain extremely close for all values of η up to approximately 0.2–0.25 T_r, differing by only 1% for $\eta = 1.0$ and by less than 0.01% at 0.25 T_r. Thereafter, the curves start to diverge more significantly, as the number of triple crossings starts to increase steadily. The onset of significant divergence occurs at the earliest time for larger values of η. The calculations suggest that for short pulse lengths ($\tau < T_r/4$), the fraction of single zero crossings is very nearly independent of the asymmetry parameter and it is not necessary to know the value of η in order to determine the fraction of spins making single zero-crossings for pulse lengths in this range. Furthermore, the fraction of spins making multiple adiabatic passages is very small and can almost be ignored. For example, the fraction of spins making two zero crossings is 0.02 for $\tau = T_r/5$ and $\eta = 0.54$.

For conditions of close to on-resonance, the avoided level crossings occur at times very close to the zero crossings, and numbers of passages are well described by the curves shown in Fig. 3. However, as δ increases, this will no longer be the case and two sets of passages are observed for off-resonance irradiation at $Q = \pm 2\delta$. The number of spins that pass through these crossings will decrease, as the irradiation frequency offset increases, and eventually drop to zero when the offset is greater than the static width of the $I = 1$ powder pattern. The fraction of spins undergoing single passages for an adiabatic-passage pulse of $T_r/3$ and $\nu_Q = 2$ MHz is plotted for three different η values as a function of δ (Fig. 4). The curves shown in (a) indicate the fraction of spins that pass once through the avoided level crossing at $Q = +2\delta$, which interconverts the $|0\rangle$ and $|-1\rangle$ eigenstates, and the $|-1\rangle$ and $|0\rangle$ eigenstates. The curves plotted in (b) show the fraction of spins which undergo a single passage through the avoided level crossings that fulfill the second condition $Q = -2\delta$ and interconvert the $|0\rangle$ and $|+1\rangle$ eigenstates and the $|+1\rangle$ and $|0\rangle$ eigenstates. The fraction of single $Q = +2\delta$ crossings declines with increased positive irradiation offsets as expected, reaching zero at $\delta = \nu_Q/2$ (i.e., 1 MHz). In contrast, the fraction of crossings also decreases with increasing negative offset, but now this fraction strongly depends on the asymmetry parameter, η, dropping to zero at $\delta = -\nu_Q(1 + \eta)/4$. The curves for the $Q = -2\delta$ condition (Fig. 4b) are mirror images of the $Q = 2\delta$ curves about δ, the strong dependence on η being observed for positive offsets. The asymmetry in the curves with $\eta < 1$ can be understood by plotting Q as a function of time during MAS. Although the time-averaged value of Q over a whole rotor period is zero, the amplitude of the maximum and minimum values of Q are not equal and are given by ω_Q and $-\nu_Q(1 + \eta)/2$, respectively. Thus, the maximum value of $|Q|$ is larger for $+Q$ than for $-Q$. This is clearly seen in the example shown in Fig. 5, where Q is plotted for the Euler angles $\alpha = 120$, $\beta = 60$ and $\gamma = 60°$ as a function of the rotor phase $\nu_r t$ for $\eta = 0.0$, 0.5, and 1.0.

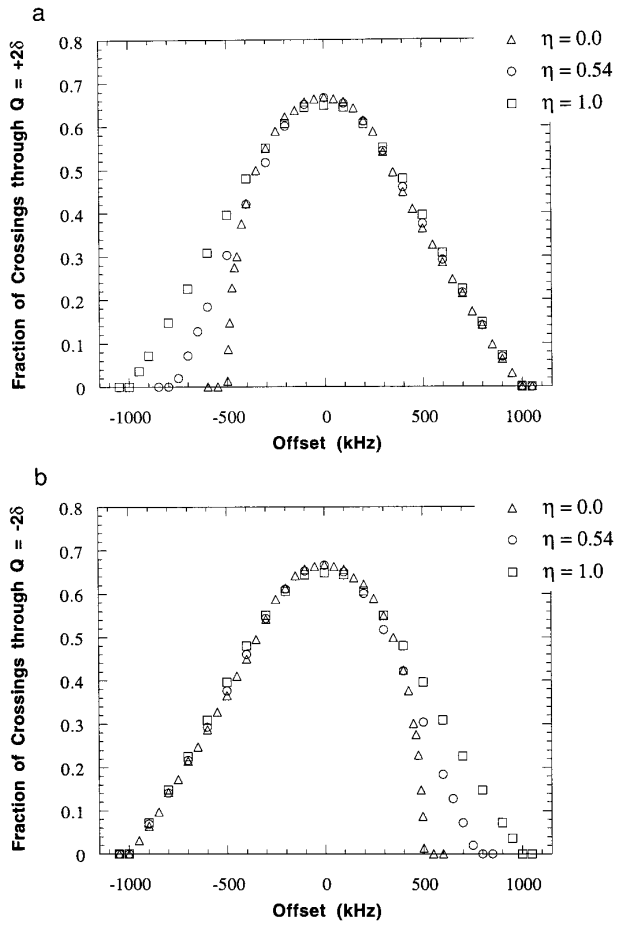

FIG. 4. The calculation of the offset dependence of the fraction of spins that undergo single crossings at (a) $Q = +2\delta$ and (b) -2δ, for an ^{14}N irradiation time of 1/3 rotor period, $\nu_Q = 2000$ kHz, and three different η values of 0.0, 0.54, and 1.0.

The asymmetries of Fig. 4 have a major effect on the population transfers. For moderate offsets, when crossings fulfilling both conditions $Q = -2\delta$ and $Q = +2\delta$ occur during the adiabatic pulse, spin populations will be converted between $|0\rangle$ and $|+1\rangle$, $|+1\rangle$ and $|-1\rangle$, and $|-1\rangle$ and $|0\rangle$. For large positive offsets ($\delta > -\nu_Q(1 + \eta)/4$), however, when the fraction of spins undergoing passages at $Q = -2\delta$ is zero, the spin populations will only be converted between $|0\rangle$ and $|-1\rangle$, and $|-1\rangle$ and $|0\rangle$. Hence, the REAPDOR fraction, measured as a function of frequency offset, is expected to show a discontinuity at $\delta = -\nu_Q(1 + \eta)/4$ and drop to zero at $\delta = -\nu_Q/2$. This should, in theory, allow us to measure both the asymmetry parameter and QCC for spin-1 nuclei. A plot of the total numbers of passages as a function of offset (from negative to

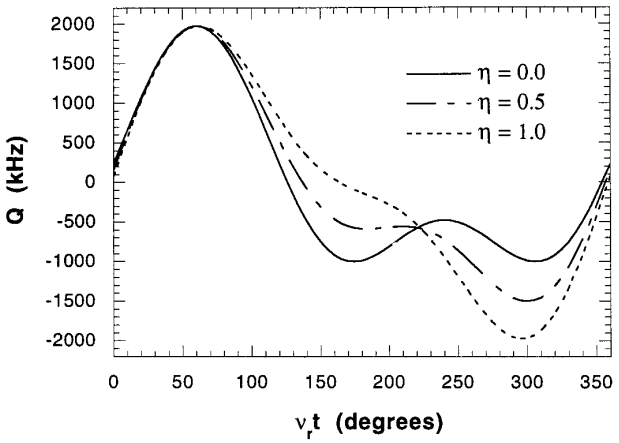

FIG. 5. A plot of the change in Q, for $\eta = 0.0$, 0.5, and 1.0, as a function of rotor phase ($\omega_r t$) for the Euler angles $\alpha = 120$, $\beta = 60$, and $\gamma = 60°$ ($\nu_Q = 2000$ kHz).

positive) will be symmetric about $\delta = 0$. Hence, the REAPDOR fraction, measured as a function of offset frequency, will also be symmetric about $\delta = 0$. Note that for small resonance frequency offsets, very little change in the number of passages is observed, and the value calculated for on-resonance irradiation provides an accurate estimate of the number of avoided level crossings.

DIPOLAR DEPHASING

The REAPDOR pulse sequence was shown in Fig. 1. During the first half of the dipolar evolution period, the ^{13}C π-pulse train causes a dipolar dephasing of the ^{13}C spins that are coupled to ^{14}N nuclei. For a particular ^{13}C–^{14}N spin pair, the average dipolar dephasing frequency, $\bar{\omega}_D^{(1)}$, during this time is

$$\bar{\omega}_D^{(1)} = m_I^{(1)} 4\sqrt{2} D \sin 2\beta \sin \alpha, \qquad [1]$$

where α and β are the polar angles that define the orientation of the ^{13}C–^{14}N internuclear vector with respect to the rotor axis, D is the dipolar coupling constant, and $m_I^{(1)}$ is the ^{14}N magnetic quantum number during the first half of the dipolar evolution period. After the adiabatic-passage pulse, changes in the ^{14}N spin states may occur. The average dipolar dephasing frequency, $\bar{\omega}_D^{(2)}$, of the ^{13}C spin during the second half of the dipolar evolution period is

$$\bar{\omega}_D^{(2)} = m_I^{(1)} 4\sqrt{2} D \sin 2\beta \sin \alpha, \qquad [2]$$

where $m_I^{(2)}$ is the ^{14}N magnetic quantum number during the second half of the dipolar evolution period. Dipolar dephasing occurs only if $m_I^{(1)} \neq m_I^{(2)}$. The changes in the ^{14}N spin states following the zero crossing are dependent on the sign of dQ/dt at the crossing and on the original spin states before the crossing (see Fig. 2). The net ^{13}C dephasing for the ^{13}C spins that are coupled to ^{14}N spins for all possible changes in spin states $|m_I^{(1)}\rangle$ to $|m_I^{(2)}\rangle$ are obtained from $\Delta\Phi = N_c T_r/2\ (\omega_D^{(1)} + \omega_D^{(2)})$. The explicit phase accumulations for the six possible eigenstate changes are

$$\Delta\Phi_1 = +N_c T_r 4\sqrt{2} D \sin 2\beta \sin \alpha \quad \text{for } |1\rangle \rightarrow |-1\rangle \qquad [3]$$

$$\Delta\Phi_2 = -N_c T_r 4\sqrt{2} D \sin 2\beta \sin \alpha \quad \text{for } |-1\rangle \rightarrow |1\rangle \qquad [4]$$

$$\Delta\Phi_3 = -N_c T_r 2\sqrt{2} D \sin 2\beta \sin \alpha \quad \text{for } |0\rangle \rightarrow |1\rangle \qquad [5]$$

$$\Delta\Phi_4 = +N_c T_r 2\sqrt{2} D \sin 2\beta \sin \alpha \quad \text{for } |1\rangle \rightarrow |0\rangle \qquad [6]$$

$$\Delta\Phi_5 = -N_c T_r 2\sqrt{2} D \sin 2\beta \sin \alpha \quad \text{for } |-1\rangle \rightarrow |0\rangle \qquad [7]$$

$$\Delta\Phi_6 = +N_c T_r 2\sqrt{2} D \sin 2\beta \sin \alpha \quad \text{for } |0\rangle \rightarrow |-1\rangle. \qquad [8]$$

Since the adiabatic-passage pulse occupies a very small fraction of the dipolar evolution time, all passages are approximated to occur instantaneously at the midpoint of the dipolar evolution period. This simplifies the calculation of dipolar dephasing tremendously. For a powder sample, the *reduced* signal intensity, S_r, at the end of the dipolar evolution period is obtained by summing over all values of α and β. The *reduced* signal is

$$S_r = \frac{1}{2\pi}\int_0^{2\pi} d\alpha \int_0^{\pi/2} \frac{1}{6}\sum_{i=1}^{6} \cos \Delta\Phi_i \sin \beta\, d\beta, \qquad [9]$$

where the value 1/6 represents the equally weighted probability that a ^{14}N spin makes one of the transitions given in Eqs. [3]–[8]. As in the REDOR experiment, the signal intensity at the end of the dipolar evolution period for a particular ^{13}C spin is given by $\cos(\Delta\Phi)$. Only the cosine projection is required since the net dipolar evolution develops symmetrically about the inspection axis in this model. The ratio of the *difference* signal, ΔS, to the *full* signal, S_o, provides a convenient measurement of the dipolar coupling and is

$$\Delta S/S_o = 1 - \frac{1}{2\pi}\int_0^{2\pi} d\alpha \int_0^{\pi/2} \frac{1}{6}\sum_{i=1}^{6} \cos \Delta\Phi_i \sin \beta d\beta. \qquad [10]$$

Implicit in Eq. [10] is the assumption that *all* ^{14}N spins make an odd number of adiabatic passages and that every ^{13}C spin is coupled to a *single* ^{14}N spin. Equation [10] is for the ideal case, which does not exist experimentally but is useful for computational purposes. Figure 3 shows that even in the adiabatic limit, only a fraction of the ^{14}N spins undergoes an odd number of zero crossings. Thus, only a fraction of the ^{13}C spins will dephase. The experimentally measured ratio of the loss in ^{13}C intensity, $\Delta S_m/S_m$, can be related to $\Delta S/S_o$ in Eq. [10] as follows. Only a fraction, ξ, of ^{14}N spins make an odd number of zero crossings and, in the adiabatic limit, only that fraction

of ^{13}C spins are dephased by the ^{13}C–^{14}N dipolar coupling. In addition, only the fraction of ^{13}C spins coupled to ^{14}N spins, ρ, may dephase. Thus, the experimentally measured ratio $\Delta S_m/S_m$ is related to $\Delta S/S_o$ by $\Delta S_m/S_m = 1/\xi\rho\ \Delta S_o/S_o$. In theory, ξ can be obtained from Fig. 3, and ρ is calculable and depends on the level of ^{13}C and ^{14}N isotopic abundance.

The orientations of the dipolar and quadrupolar principal axis systems, with respect to the rotor axis, are treated as being independent in our model. This is clearly an approximation since the particular spins in the powder that undergo the level crossings are determined by the orientation of the quadrupolar tensor with respect to the rotor frame. The subset of the powder that undergoes these crossings is unlikely to represent a uniform distribution of all possible orientations of the dipolar tensor with respect to the rotor frame. The time-averaged value of the dipolar coupling in the REAPDOR sequence may not, therefore, be the same as that obtained for calculations involving the whole powder. This will introduce a scaling in the measured dipolar coupling constant, which may introduce an error. However, one of our motivations was to develop a simple model which could be readily used to fit the experimental data. We will show in a later section that a reasonable fit between experimental and theoretical calculations can be obtained, even with this simple model.

In order to assess the size of the errors associated with ignoring the relative orientation of the dipolar and quadrupolar tensors, we performed a number of numerical simulations, using code written by S. Vega and A. Goldbourt. These computer simulations were performed by evaluating the time-dependent matrix elements of the evolution operator of the ^{13}C–^{14}N pairs during the pulse sequence. The Hamiltonian contained the quadrupolar, chemical shift, and dipole–dipole interactions and, during the pulses, RF terms were added to the Hamiltonian. A stepwise numerical integration and calculation of the expectation value of the transverse magnetization was performed. More details of the simulations will be presented elsewhere. The calculations performed using this program are discussed along with the experimental results.

EXPERIMENTAL

An alanine sample was prepared by recrystallizing 1 part [3-^{13}C, 99%] L-alanine with 20 parts [^{15}N, 95%]L-alanine (Cambridge Isotope Laboratories, Inc.). This sample has relatively isolated intramolecular ^{13}C–^{14}N spin pairs, which minimizes the effects of the intermolecular ^{13}C–^{14}N dipolar interactions. The intramolecular internuclear distance between the labeled methyl carbon and the nitrogen is 2.46 Å and corresponds to a dipolar interaction of 146 Hz. The ^{14}N QCC and η for L-alanine are 1.20 MHz and 0.26, respectively. An ^{14}N-diluted sample of glycine was also prepared by recrystallizing 1 part [1-^{13}C, 99%] glycine (Aldrich) with 20 parts [^{15}N, 99%] glycine (Isotec, Inc.). This sample is referred to as [1-^{13}C, 5%; ^{14}N, 5%] glycine. In addition, a sample of [1-^{13}C, 99%] glycine was also used in some experiments (no ^{14}N dilution). Values for the QCC, η, the intramolecular internuclear distance, and the ^{13}C–^{14}N dipolar coupling of 1.18 MHz, 0.54, 2.49 Å, and 141 Hz have been determined for glycine, respectively (*15*).

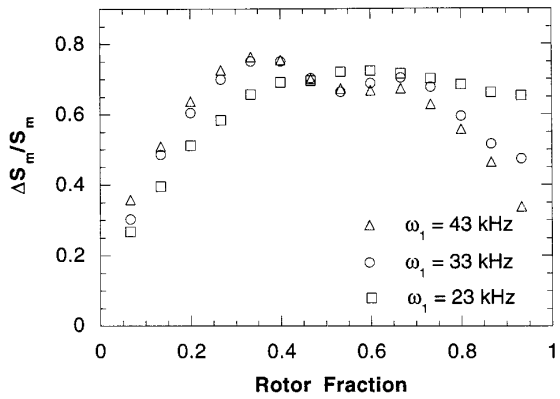

FIG. 6. The experimental dependence of the REAPDOR $\Delta S_m/S_m$ values on the length of the ^{14}N irradiation pulse, for three different ^{14}N RF fields of 43, 33, and 23 kHz. Values of $\Delta S_m/S_m$ were obtained for the carboxyl carbon of [1-^{13}C, 99%] glycine for $N_c = 10$, a spinning speed of 1.5 kHz, and an ^{14}N irradiation offset of 14.5 kHz.

The NMR experiments were performed with two spectrometers. The system used for the alanine experiments consists of a homebuilt triple-channel spectrometer equipped with a Tecmag Libra pulse programmer and a 3.55 T magnet (i.e., a 150-MHz system). The homebuilt triple-channel MAS probe used a Chemagnetics 7.5-mm spinning head and the transmission-line design of McKay. The spinning speed was set to 3125 Hz and stabilized to within 2 Hz by a homebuilt spinning speed controller. Adiabatic-passage pulses were applied 50 kHz off-resonance (referenced to the ^{14}N resonance of alanine in solution) with RF field strengths ranging from 18 to 50 kHz. The ^{13}C RF field strength of 33.8 kHz was used for the cross-polarization and the π-pulse train. Proton decoupling was performed with an RF field strength of 110 kHz. A CMX-360 spectrometer was used for the glycine experiments. This instrument is equipped with a triple resonance Chemagnetics probe with 5-mm zirconia rotors. Spinning speeds of 1.5 and 3.0 kHz were used and stabilized to within 1 and 2 Hz, respectively. Radio-frequency field strengths of 23 through 43 kHz (^{14}N) and 62.5 kHz (^{13}C and ^{1}H) were employed.

RESULTS AND DISCUSSION

Experiments were performed to explore the effect of the ^{14}N irradiation time on the REAPDOR dipolar dephasing signals. Figure 6 shows the dependence of the measured REAPDOR ratio $\Delta S_m/S_m$ on the ^{14}N adiabatic pulse length for [1-^{13}C, 99%] glycine. Results for three different ^{14}N RF field strengths $\nu_1 = 23$, 33, and 43 kHz are shown. The shape of the experimental curves resembles the calculated odd number of zero crossing curves shown in Fig. 3. $\Delta S_m/S_m$ increases rapidly with

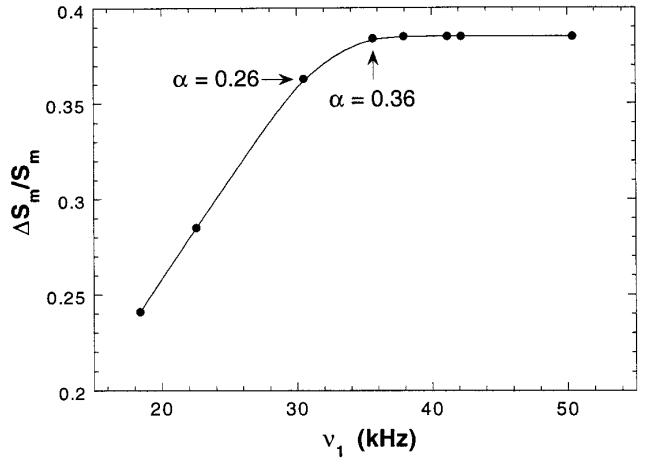

FIG. 7. The experimental dependence of the REAPDOR $\Delta S_m/S_m$ values on the ^{14}N RF field strength (expressed in kilohertz) for [3-^{13}C]L-alanine. The ^{14}N RF field was applied 50 kHz off resonance, for $\tau = 3T_r/16$; $N_c = 18$ and $\nu_r = 2$ kHz.

the adiabatic pulse length and reaches a maximum at $T_r/3$ for the higher RF powers (33 and 43 kHz). However, the curves of $\Delta S_m/S_m$ are not symmetric about $T_r/2$, as would be predicted from inspection of Fig. 3b, and $\Delta S_m/S_m$ does not zero after a complete rotor period of irradiation. There are two reasons for this. First, increasing numbers of multiple zero crossings occur with a longer adiabatic pulse; hence, some of the multiple zero crossings fail to return the spin system to its original state if the adiabatic condition is not fulfilled. Second, for longer adiabatic-passage pulse lengths, the approximation that all the changes in spin populations occur at the midpoint of the pulse becomes less reasonable. In fact, for an adiabatic-passage pulse length equal to one rotor period, the N_c-rotor-cycle REAPDOR experiment effectively becomes a one-rotor-cycle TRAPDOR experiment. Consequently, there should be a net dipolar dephasing for the $\tau = T_r$ REAPDOR experiment. The higher the RF power, the higher the value for α, and the closer the shape of the curve mimics that of the theoretically calculated curve. For short ^{14}N irradiation, conditions where single ^{14}N crossings predominate, little difference is observed between the curves obtained with RF field strengths of 33 kHz and 43 kHz. However, upon reducing the RF field strength to 23 kHz, a noticeable reduction in $\Delta S_m/S_m$ is observed. Radio-frequency field strengths of 23, 33, and 43 kHz correspond to α values of 0.2, 0.4, and 0.7, respectively, for a MAS spinning speed at 1.5 kHz. Thus, experimentally, α values as low as 0.4 appear to result in close-to-adiabatic passages. As long as short ^{14}N pulses are used, the REAPDOR fractions are not strongly affected by changes in α, even down to relatively low values. At longer irradiation times, where multiple passages occur, any errors due to nonadiabatic passages can accumulate, and a divergence in the curves obtained with values for α of 0.4 and 0.7 is seen, higher values of $\Delta S_m/S_m$ being observed for the curve with $\alpha = 0.4$. For the low $\alpha = 0.2$ value, the curve deviates considerably from expectations and $\Delta S_m/S_m$ increases steadily with increased irradiation time, reaching a maximum after more than half a rotor period of irradiation; thereafter, only a small decrease in $\Delta S_m/S_m$ is observed. For such low values of α, each zero crossing results in only a small interconversion of ^{14}N populations, but the amount of the population transfer increases with each crossing, resulting in a greater REAPDOR effect as τ increases. This effect is difficult to quantitate and, consequently, may not be so readily utilized.

Figure 7 shows the dependence of $\Delta S_m/S_m$ on the ^{14}N RF field strength for the alanine sample for $\nu_r = 2$ kHz and $\tau = 3T_r/16$. The value of $\Delta S_m/S_m$ increases steadily with increased RF field strengths, reaching a maximum at approximately 35 kHz, whereafter the dipolar dephasing remains constant. An RF field strength of 35 kHz and a spinning speed of 2 kHz corresponds to a value for α of 0.36, and again, this shows that close-to-adiabatic conditions appear to be met for ^{14}N for adiabatic parameters as low as 0.36. However, below a value for α of approximately 0.26 the values of $\Delta S_m/S_m$ are very sensitive to the RF field strength.

Experiments were also performed on [1-^{13}C, 99%] glycine, to explore the effect of ^{14}N irradiation offset on the REAPDOR signals. An RF field strength of 43 kHz, $N_c = 10$, and a spinning speed of 1.5 kHz were used in these experiments. Figure 8 shows the adiabatic-passage pulse length dependence of $\Delta S_m/S_m$ for offsets of 0.0, 14.5, and 40 kHz (measured relative to the ^{14}N resonance of an aqueous glycine solution). Larger REAPDOR fractions are observed for the on-resonance experiment, for short irradiation times, and for irradiation times close to a full rotor period in comparison to off-resonance data. This is presumably due to the irradiation of the double quantum transition (*16*). The ^{14}N double quantum transition of solid glycine is shifted to higher frequencies and broadened, relative to the ^{14}N resonance of aqueous glycine, due to the second-order quadrupolar interaction: In a magnetic field strength of 8.46 T, the double quantum transition powder pattern spreads

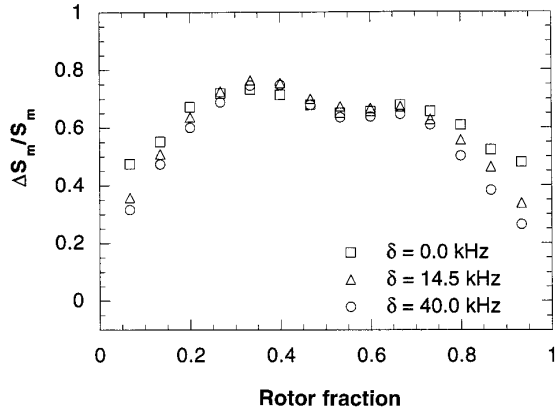

FIG. 8. The experimental dependence of the REAPDOR $\Delta S_m/S_m$ values of [1-^{13}C, 99%] glycine on the ^{14}N irradiation length, for three different ^{14}N offset values of 0.0, 14.5, and 40.0 kHz. ($N_c = 10$, $\nu_r = 1.5$ kHz, and $\nu_1(^{14}N) = 43$ kHz.)

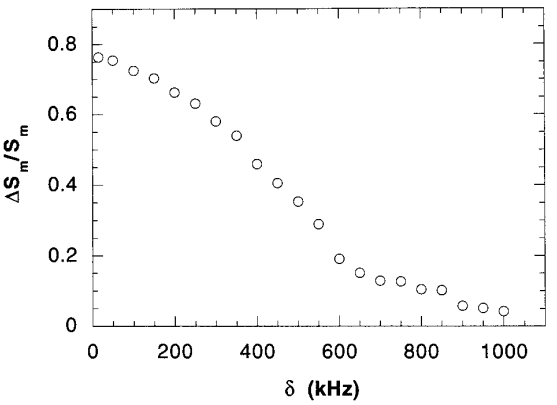

FIG. 9. The offset dependence of the REAPDOR $\Delta S_m/S_m$ signals of [1-^{13}C, 99%] glycine, for an ^{14}N irradiation time of 1/3 rotor period. ($N_c = 10$, $\nu_r = 1.5$ kHz, and $\nu_1(^{14}N) = 43$ kHz.)

from +0.3 to +4 kHz, relative to aqueous glycine (*5*). Therefore, irradiation at $\delta = 0$ kHz will result in a partial excitation of this transition and a partial mixing of the $|+1\rangle$ and $|-1\rangle$ populations. These results suggest that the offset should be chosen to avoid the double quantum transition, in order to obtain predictable population transfers. Effects caused by irradiation of the double quantum transition will be less significant for the larger second-order quadrupolar broadenings that occur at lower fields and larger quadrupolar coupling constants.

Our calculations suggested that the REAPDOR experiment could be used to measure the ^{14}N asymmetry parameter and the quadrupolar coupling constant by measuring $\Delta S_m/S_m$ as a function of ^{14}N offset. Figure 9 shows the dependence of $\Delta S_m/S_m$ on the ^{14}N RF offset for [1-^{13}C, 99%] glycine obtained by using an ^{14}N irradiation time of $T_r/3$. For glycine, the ^{14}N QCC is 1.18 MHz and η is 0.54; thus, discontinuities in the $\Delta S_m/S_m$ profile are predicted to occur at $\delta = \pm 681$ kHz and ± 885 kHz. A clear discontinuity is observed at 650 $\pm$ 50 Hz and $\Delta S_m/S_m$ falls below 0.1 between 850 and 900 Hz. The sudden decrease in $\Delta S_m/S_m$ between 850 and 900 Hz is reproducible and is most likely a consequence of the singularity in the ^{14}N powder pattern. A value for ω_Q of 875 $\pm$ 25 kHz is determined from these data. The experimental results and the theoretical predictions are in reasonable agreement. Thus, the offset-dependent REAPDOR experiment provides an indirect method of measuring the coupling constants and asymmetry parameters for $I = 1$ quadrupolar nuclei. However, a small REAPDOR fraction (<0.05) is observed out to an offset of 1 MHz, and the off-resonance RF field for $\delta > 885$ Hz still results in a very small (but close to negligible) REAPDOR fraction. This may result in a source of error in the measurement of ω_Q of approximately 10%, if no discernible ''cutoff'' can be distinguished. This error will, however, diminish for larger QCCs. Furthermore, an estimate for η will become difficult, unless a clear discontinuity is visible in the curve obtained as a function of offset.

Finally, measurement of heteronuclear dipolar couplings between isolated spin-1/2 and spin-1 nuclear pairs is illustrated. Theoretical and experimental REAPDOR data for the ^{14}N-diluted [1-^{13}C, 5%; ^{14}N, 5%] glycine sample are plotted as a function of the dimensionless parameter $\lambda = N_c T_r D$ in Fig. 10. The experimental data are plotted assuming a dipolar coupling constant, D, of 141 Hz. The theoretical values of $\Delta S/S_0$ are calculated from Eq. [10]. The measured $\Delta S_m/S_m$ were obtained with spinning speeds of 1.5 and 3.0 kHz and with an ^{14}N adiabatic-passage pulse length of $T_r/3$ applied 14.5 kHz off-resonance. Slightly larger values of $\Delta S_m/S_m$ are obtained for the lower spinning speed. This is consistent with the larger value of α (0.7) calculated for a spinning speed of 1.5 kHz. Comparison of the experimental data with the theoretical dephasing curve requires corrections mentioned earlier. In particular,

$$\Delta S/S_0 = (1/\rho\xi\epsilon)\Delta S_m/S_m, \qquad [11]$$

where ϵ is now introduced as a parameter to quantify the effectiveness of the adiabatic passages. Perfect adiabatic passages are indicated by $\epsilon = 1$, and deviations from 1 indicate inefficient adiabatic transfers of populations among the eigenstates, or other sources of errors. A value for ξ of 0.667 was obtained from Fig. 3b for an adiabatic-passage pulse of duration $T_r/3$. The fraction of ^{13}C–^{14}N spin pairs, ρ, is 0.816 for this sample. The experimental data can be fit to the theoretical curve with values for ϵ of 1.04 and 0.92 for $\nu_r = 1.5$ and 3.0 kHz, respectively. The data are then in close agreement with the predicted REAPDOR curve calculated assuming ideal adi-

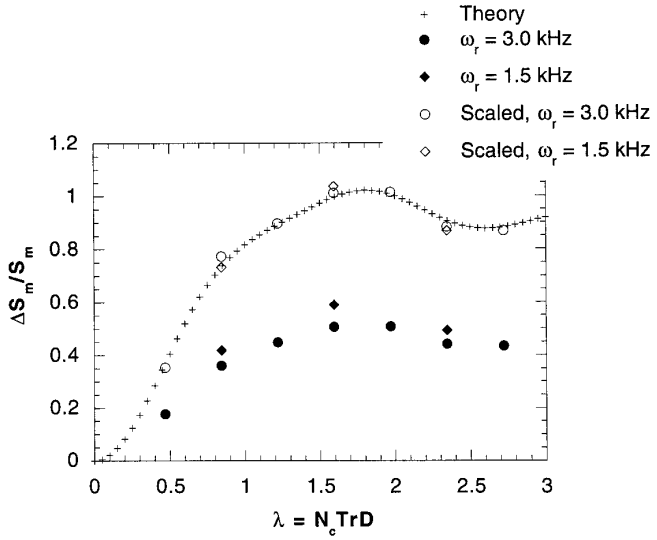

FIG. 10. Theoretical and experimental REAPDOR dipolar dephasing curves for [1-^{13}C, 5%; ^{14}N, 5%] glycine plotted as function of λ, for two different spinning speeds of 3.0 and 1.5 kHz. ($\nu_1(^{14}N) = 43$ kHz; $\delta(^{14}N) = 14.5$ kHz.) Experimental values of $\Delta S_m/S_m$ were scaled according to Eq. [11] (see text) (open circles) to allow comparison with the calculated values of $\Delta S_m/S_o$ (crosses).

abatic passages. As α decreases, ϵ decreases. This is consistent with theoretical predictions: Fewer spins are transferred between eigenstates when the experimental conditions are further from the adiabatic limit. Importantly, even for values of α as low as 0.35, the shape of the dipolar dephasing curve is very close to that of the theoretical one and only the magnitude of $\Delta S_m/S_m$ is affected. The experimental data can be fitted to the ideal REAPDOR curve by employing only one variable parameter: the simple scaling factor ϵ.

Figure 11a shows REAPDOR experimental results for the ^{14}N-diluted alanine sample obtained with an adiabatic passage pulse of half a rotor period. The experimental data, plotted assuming $D = 141$ Hz, are compared with both the idealized dephasing curve $\zeta\Delta S/S_o$ (solid line) and data generated from numerical computer simulations (dashed lines) (see later discussion), where the idealized dephasing curve ($\Delta S/S_o$) obtained from Eq. [10] has been scaled by the fraction of spins making an odd number of passages ρ (0.614). The experimental data ($\Delta S_m/S_m$) have also been scaled by the number of ^{13}C–^{14}N spin pairs ρ (0.822), to account for the number of uncoupled nuclei. The experimental alanine data (solid circles) show stronger dephasing than the idealized dephasing curve of Eq. [10] would predict. Once again, it is also possible to scale the idealized curve with an efficiency parameter $\epsilon = 1.1$, resulting in a good fit between experimental and calculated dephasing (Fig. 11b). A value of $\epsilon > 1$ indicates that dephasing observed experimentally is slightly larger than predicted and is presumably an indication that the passages are not perfect, and suggests that the interconversion of populations between eigenstates is increased by multiple passages. Experiments were repeated with a shorter adiabatic pulse of $T_r/5$, and these data (not shown) fit the idealized curve quite well with $\epsilon = 1.0$, providing further evidence that the errors due to nonadiabatic passages increase with increasing τ.

An important observation that can be made from these experimental results is that short adiabatic-passage pulses produce dipolar dephasing that is well described by Eq. [10] and, for modest quadrupolar interactions, is described by $\epsilon = 1.0$ (e.g., $\epsilon \approx 1$ for the slow-spinning glycine and for the short adiabatic-passage pulse-length alanine experiments). This ideal situation occurs because slow spinning makes the adiabatic condition more likely and short pulse lengths nearly eliminate multiple passage attempts. However, ϵ is noticeably different from unity for the $\nu_r = 3.0$ kHz, $\tau = T_r/3$ glycine, and for the $\nu_r = 3.125$ kHz, $\tau = T_r/2$ alanine experiments, with $\epsilon = 0.92$ and 1.1 for the glycine and alanine data, respectively. A simple picture using the results in Figs. 3 and 7 and the likely fact that we are at the edge of the adiabatic condition for the fast spinning data can explain the differences in ϵ. For $\tau = T_r/3$, spins mostly attempt single passages, but some spins also attempt double passages; for $\tau = T_r/2$, in addition to the single-passage attempts, a significant fraction of spins now attempt double passages. For the $\tau = T_r/3$ pulse, a fraction of the spins attempting a single passage do not make the transition and these spins do not cause dipolar dephasing. Similarly, a fraction of those attempting double passages do not return to their original states, either, and these will cause dipolar dephasing. However, since the fraction of spins attempting double passages is small, there are not enough failed double passages to make up for the lack of single passages. Thus, the fraction of spins making a single transition is less than

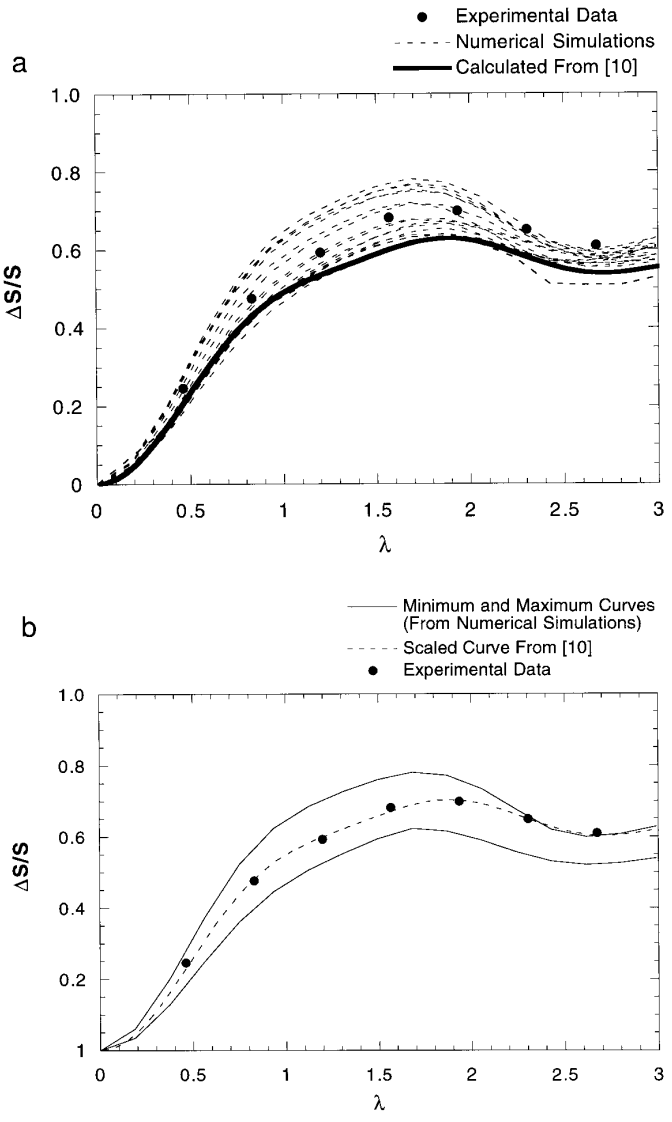

FIG. 11. The REAPDOR dipolar dephasing curves obtained for [3-^{13}C]L-alanine, with ^{14}N adiabatic pulses of $T_r/2$, as a function of λ. (a) The experimental values of $\Delta S_m/S_m$ have been scaled by $1/\rho$, where $\rho = 0.822$, to allow direct comparison with the calculated value of $\zeta\Delta S/S_o$ (solid line) from [10] ($\zeta = 0.614$). The data are plotted with together with results obtained from numerical simulations with random orientations of the CSA, quadrupolar, and dipolar tensors. (b) Curves representing simulated curves showing the minimum and maximum amount of dephasing are shown together with the experimental data ($\Delta S_m/S_m\rho$), and the adjusted idealized curve $\zeta\epsilon\Delta S/S_o$ (where the idealized dephasing curve has been scaled with the efficiency parameter, $\epsilon = 1.1$). ($\nu_1(^{14}\text{N}) = 40$ kHz, $\delta = 50$ kHz, and $\nu_r = 3.125$ kHz.)

that expected ideally (i.e., $\epsilon < 1$) for these conditions. However, for $\tau = T_r/2$ it is possible that the fraction of spins not making the expected single passage can be compensated by the fraction of spins not making their expected double passages, since the double passage fraction is quite large. Consequently, the fraction of spins making a single passage can exceed the theoretically expected fraction. Those spins that do not make a double passage cause dipolar dephasing. Thus, for $\tau = T_r/2$ it is possible to fine $\epsilon > 1$.

An encouraging finding is that the experimental data from both alanine and glycine can be fit to the same simple theory no matter the value of ϵ, allowing internuclear distances to be obtained. The data from glycine are for the carboxyl carbon, whereas the data for alanine are for the methyl carbon; the orientation of the dipolar and quadrupolar tensors in these two samples are different. Our theoretical idealized model does not take this into account, yet the shape of the experimental curves is unaffected.

Numerical computer simulations of the REAPDOR experiment were performed for the alanine data acquired with an adiabatic pulse length of $T_r/2$, in order to obtain more insight into the causes of the disagreement between the curves calculated with Eq. [10], and to explore the sources of the errors. Twenty-five simulations were performed using the known the values for the ^{14}N QCC and η, and the CSA of the methyl group of alanine. These simulations differed only in the relative orientations of the quadrupolar, chemical shift, and dipolar tensors. These orientations were chosen at random. A random selection of these simulations is shown by dashed lines in Fig. 11a. One nonrandom set of orientations was also chosen, namely one where the dipolar and quadrupolar tensors are collinear. All curves calculated from the numerical simulations lie in a thick band varying by about $\pm 0.1 \Delta S/S_0$ for $\lambda = 1.5$, and the experimental alanine data fall within this band. The idealized dephasing curve (solid line) (from Eq. [10]) lies near the bottom of the band of the simulated data. The only curve that has significantly lower values of $\Delta S/S_0$ for $\lambda > 2$ than those of the idealized dephasing curve results from the numerical simulation with collinear quadrupolar and dipolar tensors. Furthermore, the maximum values of $\Delta S/S_0$ were obtained for numerical simulations with very different orientations of the principal axes of the quadrupolar and dipolar tensors; however, some exceptions to this rule were noted, where tensors with large relative orientations also resulted in smaller values of $\Delta S/S_0$. Most noteworthy, however, is the fact that all these curves are characterized by a shape which is very similar to the idealized one.

The idealized dephasing curve is calculated by making the simple assumption that the dephasing is independent of the relative orientation of the ^{13}C–^{14}N spin pair and the ^{14}N quadrupolar tensor. In addition, this curve assumes that all passages are adiabatic. We can conclude from the numerical simulations that the REAPDOR dephasing does depend on the relative orientations of the quadrupolar, chemical shift, and dipolar tensors. Furthermore, the simulations suggest that part of the correction factor ϵ that was included in Eq. [11] is due in part to our neglect of the effect of the relative tensor orientations in our simple model. Different orientations of these tensors will alter both the average dipolar coupling during the sequence *and* the part of the powder that undergoes the passages. Since the adiabaticity parameter for each spin α', which governs how efficient each passage is, varies throughout the powder, a change in subset of spins undergoing the passages should also result in differences in dephasing, especially for values of α (the adiabaticity parameter for the powder) close to, but not in, the adiabatic regime. Importantly, however, this dependence on relative orientation is not so strong as to completely eliminate the possibility of obtaining internuclear distances. Figure 11b shows curves representing the minimum and maximum amount of dephasing calculated numerically, together with the experimental data. If either of these curves is used to fit the experimental data between $\lambda = 0$ and 1.5 (i.e., before an oscillation is observed), by varying the dipolar coupling and hence λ, an uncertainty in the internuclear distance of no more than $\pm 5\%$ is obtained.

Finally, the dephasing of the spin-1/2 signal at the end of the rotor period in the TRAPDOR experiment (*5*, *6*) depends on both the relative orientation of the dipolar tensor to the rotor axis, and the times in the rotor period where the zero crossings in Q occur. Thus, the dephasing observed in TRAPDOR experiment also depends on the relative orientation between the quadrupolar coupling tensor and the heteronuclear dipolar tensor, and this information is required to determine internuclear distances accurately in the TRAPDOR experiment. This information is not required in our simple model used to analyze the REAPDOR data, because of the approximation that all single passages occur at the midpoint of the ^{14}N pulse. This was considered justified because the adiabatic-passage pulse occupies such a short time in the dipolar evolution period (typically less than 3% of the total evolution time). The fact that there are correlations between the spins that undergo the adiabatic passages and the dipolar evolution of the coupled ^{13}C spins in the REAPDOR experiment appears to be a far less serious approximation than if this is neglected in the TRAPDOR experiment. The good agreement between the experimental results and the theoretical REAPDOR dipolar dephasing curves for both the glycine and alanine samples suggests that this information is not necessary to allow at least approximate estimates of the dipolar couplings to be extracted from REAPDOR data, for modest QCCs. The preliminary numerical simulations presented in this paper are in agreement with this and have shown that the REAPDOR experiment is relatively insensitive to the relative orientation between the dipolar and quadrupolar tensors. However, some changes in the dephasing curves with different tensor orientations were apparent (Fig. 11): Without any knowledge of the relative orientations of the tensors, the experimental data could be fit with an error of $\approx \pm 5\%$ in the

internuclear distance. Clearly, more numerical simulations are required to explore the differences between the idealized and calculated curves not only for different orientations, but also for larger asymmetry parameters and larger QCCs. These simulations would help assess our ability to calculate internuclear distances accurately for a wider range of systems.

CONCLUSIONS

The model developed in this paper allows experimental REAPDOR dipolar dephasing curves to be simulated for a relatively wide range of experimental conditions, for systems with moderate QCCs, allowing $^{13}C/^{14}N$ internuclear distances to be extracted. Use of a short ^{14}N pulse of one-quarter of a rotor period, or less, minimizes the number of multiple passages and ensures a closer fit between experiment and theory. Internuclear distances can be obtained, even under conditions where the ^{14}N passages are no longer close to being adiabatic ($\alpha \approx 0.3$), by applying a simple scaling factor to the experimental data. Two different avoided level crossings occur for off-resonance ^{14}N irradiation. The dependence of the crossings on η, combined with a sharp cutoff in the REAPDOR fraction when the ^{14}N irradiation is applied outside the limits of the first-order ^{14}N powder pattern, allows the ^{14}N QCC and η to be determined.

ACKNOWLEDGMENTS

Support from the NSF to C.P.G. through the National Young Investigator program (DMR-9458017) and for Grant CHE-9405436 to purchase the CMX-360 NMR spectrometer is gratefully acknowledged. T.G. thanks the NSF for partial support of this work through CHE-9796188 and acknowledges the donors of the Petroleum Research Fund, administered by the American Chemical Society, for partial support of this research. Shimon Vega and Amir Goldbourt are thanked for providing the computer program used for the numerical simulations and for stimulating discussions.

REFERENCES

1. T. Gullion, *Chem. Phys. Lett.* **246,** 325 (1995).
2. T. Gullion, *J. Magn. Reson.* **A117,** 326 (1995).
3. T. Gullion and J. Schaefer, *J. Magn. Reson.* **81,** 196 (1989); T. Gullion and J. Schaefer, *in* ''Advances in Magnetic Resonance'' (W. S. Warren, Ed.), Vol. 13, p. 57, Academic Press, New York (1989).
4. J. R. Garbow and T. Gullion, *J. Magn. Reson.* **95,** 442 (1991).
5. C. P. Grey and W. S. Veeman, *Chem. Phys. Lett.* **192,** 379 (1992).
6. C. P. Grey, A. J. Vega, and W. S. Veeman, *J. Chem. Phys.* **98,** 7711 (1993).
7. C. P. Grey and A. J. Vega, *J. Am. Chem. Soc.* **117,** 8232 (1995).
8. A. J. Vega, *J. Magn. Reson.* **96,** 50 (1992).
9. A. J. Vega, *Solid State Nucl. Magn. Reson.* **1,** 17 (1992).
10. J. Haase, M. S. Conradi, C. P. Grey, and A. J. Vega, *J. Magn. Reson.* **A109,** 90 (1994).
11. C. P. Grey, A. P. A. M. Eyckelboom, and W. S. Veeman, *Solid State. Nucl. Magn. Reson.* **4,** 113 (1995).
12. H.-M. Kao and C. P. Grey, *J. Phys. Chem.* **100,** 5105 (1996).
13. A. J. Vega and C. P. Grey, unpublished results.
14. M. M. Maricq and J. S. Waugh, *J. Chem. Phys.* **70,** 3300 (1979).
15. R. A. Haberkorn, R. E. Stark, H. van Willigen, and R. G. Griffin, *J. Am. Chem. Soc.* **103,** 2534 (1981).
16. R. Eckman, L. Mueller, and A. Pines, *Chem. Phys. Lett.* **74,** 376 (1980).
17. L. Chopin, C. P. Grey, and T. Gullion, in preparation.